







## Cross-Section Calculation and Comparative Assessment of Al and Zr as Cladding for NIRR-1

Olumide O. Ige<sup>1</sup>, Abel B. Olorunsola<sup>2</sup>, Emmanuel J. Adoyi<sup>1</sup>, Omolayo M. Ikumapayi<sup>3,4\*</sup>,  
Opeyeolu T. Laseinde<sup>3</sup>

<sup>1</sup> Department of Physics, Nigeria Defense Academy, Kaduna 800281, Nigeria

<sup>2</sup> Department of Physics, Federal University of Lafia, Lafia 950101, Nigeria

<sup>3</sup> Department of Mechanical and Industrial Engineering Technology, University of Johannesburg, Johannesburg 2092, South Africa

<sup>4</sup> Department of Mechanical and Mechatronics Engineering, Afe Babalola University, Ado Ekiti 360101, Nigeria

Corresponding Author Email: [ikumapayi.omolayo@abuad.edu.ng](mailto:ikumapayi.omolayo@abuad.edu.ng)

Copyright: ©2024 The authors. This article is published by IETA and is licensed under the CC BY 4.0 license (<http://creativecommons.org/licenses/by/4.0/>).

<https://doi.org/10.18280/mmep.110929>

### ABSTRACT

**Received:** 2 March 2024

**Revised:** 9 May 2024

**Accepted:** 15 May 2024

**Available online:** 29 September 2024

#### Keywords:

NIRR-1, LEU, cladding, cross section, EMPIRE 3.2.3

The NIRR-1 went through conversion from highly enrich uranium HEU to low enriched Uranium LEU fuel. The design of the fuel core is such that the cladding materials have been changed from aluminum to zirconium. The cladding materials may likely experience neutron dose which is susceptible to degradation of the materials. Hence, the needs to ascertain the level of degradation of the materials are crucial. Therefore, we calculate the reaction cross section of Al and Zr target with EMPIRE 3.2.3 modular nuclear reaction code. The calculated results were compared with measured data from EXFOR and the Evaluated Nuclear Data (ENDF). Comparative assessment of neutronic impact of Al and Zr used in the high and low enrich uranium fuel in NIRR-1 were carry out by compared cross section of Al with Zr results in the reaction channel relevance to the cladding materials. The results show that  $^{90}\text{Zr}(n,el)$  have high mean cross section of 1720.30 mb and  $^{90}\text{Zr}(n,\gamma)$  with lower mean cross section of 0.54 mb while  $^{27}\text{Al}(n,p)$  and  $^{27}\text{Al}(n,\gamma)$  high and low mean cross section is 482.5 mb and 0.022 mb respectively. It was observed that Zr target absorption cross section is better compared to Al target. This indicates that Zr has proven higher resistance to corrosion and longevity in terms of degradation as cladding materials.

## 1. INTRODUCTION

The Nigerian Research Reactor-1 (NIRR-1) is a miniature Neutron Source Reactors (MNSRS) type, sited at the Centre for Energy Research and Training (CERT), Ahmadu Bello University (ABU), Zaria, Nigeria. The reactor was designed and manufactured by the Institute of Atomic Energy (CIAE), Beijing, China; primarily for Neutron Activation (NAA), production of short-lived radioisotopes, and also for the training of nuclear engineers and technicians [1]. The NIRR-1 was utilized for neutron activation analysis after its operation in 2004 [2]. It is obvious that the reactor NIRR-1 went through conversion from Highly enriched Uranium HEU to Low enriched Uranium LEU fuel under the International Atomic Energy Agency [3] in collaboration with the CIAE, aims to minimize and when possible, eliminate potentially weapon-useable nuclear material associated with the HEU around the globe; and to achieve non - proliferation and threat reduction. This conversion required a new low enrichment fuel qualified for use in this reactor and the operation with LEU fuel involved major changes in the compartment most especially fuel cladding materials and others, which in turn may affect

the neutronic characteristics of the reactor. The major replaceable parameters are displayed in Table 1.

Neutron induced reaction cross section on zirconium target is used to simulate and explored advanced reactors in nearly all commercial water reactors as fuel rod cladding. But the experimental data are scanty or grossly not in existence. There also, exists conflicts in nuclear data evaluator between, JEFF and JENDL in cross section at higher neutron energies for all channels [4].

Calculations of neutron-induced reaction cross-section on  $^{27}\text{Al}$  and  $^{90}\text{Zr}$  were based on the reaction channel of importance to cladding such as  $(n,el)$ ,  $(n,\gamma)$ ,  $(n,p)$ , and  $(n,2n)$  with the help of modular statistical code EMPIRE 3.2 [4-6] which includes the theoretical models and the parameter testing to obtain cross-section in good agreement with the available and consistency with available experimental data retrieved from EXFOR [7] and benchmarking with existing evaluated nuclear data. The calculated values were used to conduct the comparative assessment of the cross-section of Al and Zr, with this study one could tell the rate of neutron absorption.

**Table 1.** Parameters of core design of NIRR-1 LEU compared with HEU [4, 5]

Parameter	LEU	HEU
Cold excess reactivity $mk$	3.94	4.97
Material of the rods/grid plate	Zircaloy – 4	Al
Materials for dummy elements	Zircaloy – 4	Al
Number of dummy elements	15	3
Number of active rods	335	347
Cladding material	Zircaloy - 4	Al -alloy (303 -1)
Wt % U in fuel meat	88%	28%
Density of fuel meat $g/cm^3$	10.56	3.456
Rated thermal power	34 kW	30 kW
U-235 enrichment, wt %	13 %	90.2 %
U – 235 total core loading, g	1410.90 g	1006.65 g
Fuel meat	UO <sub>2</sub>	U – Al <sub>4</sub>

**2. MODEL AND PARAMETERS**

In this study, we adopted the parametrization by varying parameters to match the available and consistent experimental data retrieved from EXFOR using EMPIRE 3.2 code [8, 9]. The code accounts for the major nuclear reaction mechanisms such as optical direct, compound nucleus, and pre-equilibrium model. Optical model parameters OMP was calculated up the discrete levels to for incident and outgoing reaction channel for elastic and absorption cross section. The optical model parameters were taken from the RIPL-3 library [10]. Hofman, Richert, Tepel, and Weidenmueller (HRTW) model was implemented for the reaction between the projectile and the target nucleus to form compound nucleus, subsequently, emits a gamma ray compensated with width fluctuation correct factor. Exciton model in term of the Iwamoto – Harada model [11] which account for the formation of a cluster probability of exciton below and above the Fermi surface were implemented and Kalbach [12] method was also implemented for the nucleon emission rate calculation [12]. The mean free path parameter in PCROSS is set to 2.0. The compound nucleus CN decay and direct cross sections were added inherently. CN anisotropy was calculated using Blatt-Biedenharn coefficient [13].  $\gamma$  – ray transition formalism is based on Giant Dipole Resonance GDR parameters which are taken from the compiled experiment contained in RIPL-3 [14]. The gamma-ray transmission coefficients are gotten from the

gamma-ray strength function of Kopecky and Uhl formalism [15].

**3. RESULTS AND DISCUSSION**

The calculated results of  $^{27}Al(n, 2n)$ ,  $^{27}Al(n, el)$ ,  $^{27}Al(n, p)$  and  $^{27}Al(n, \gamma)$  cross section is displayed in Figures 1-4. The theoretical calculation from EMPIRE 3.2.3 was in good agreement with the experimental data obtained from references [16-18] as shown in Figure 1. It is noted that the cross section increases with an increase in incident neutron energy while variation exist between the existing evaluated data and our calculated results. The results of  $^{27}Al(n, el)$  cross section is displayed in Figure 2. The cross section was almost constant with increase in incident energy while reproducing the experimental data [19, 20] and also in good harmony with existing evaluated nuclear data file. In Figure 3,  $^{27}Al(n, p)$  cross section decreases with increase in energy, but our results reproduce experimental data [21] and closed to Mannhart et al. [22] data but discrepancy exists between the evaluated nuclear data. Neutron induced reaction of  $^{27}Al(n, \gamma)^{28}Al$  cross section is presented in Figure 4. Both the calculated result and existing evaluated nuclear data remained constant with increase in incident energy throughout the study energy region. This may likely be to do with deficiency in models used as a result of lack of experimental data to constrain the model.

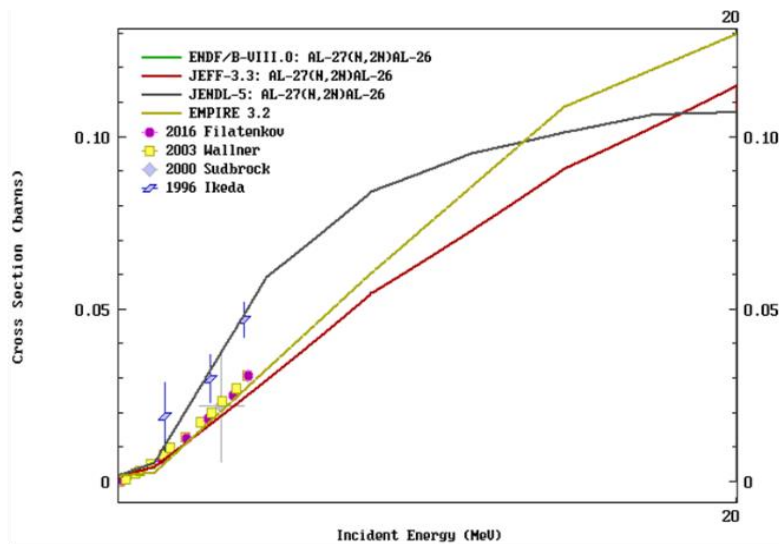


**Figure 1.** Calculated reaction cross-section with EMPIRE 3.2.3 on  $^{27}Al(n, 2n)$  in comparison with the measured data evaluated data

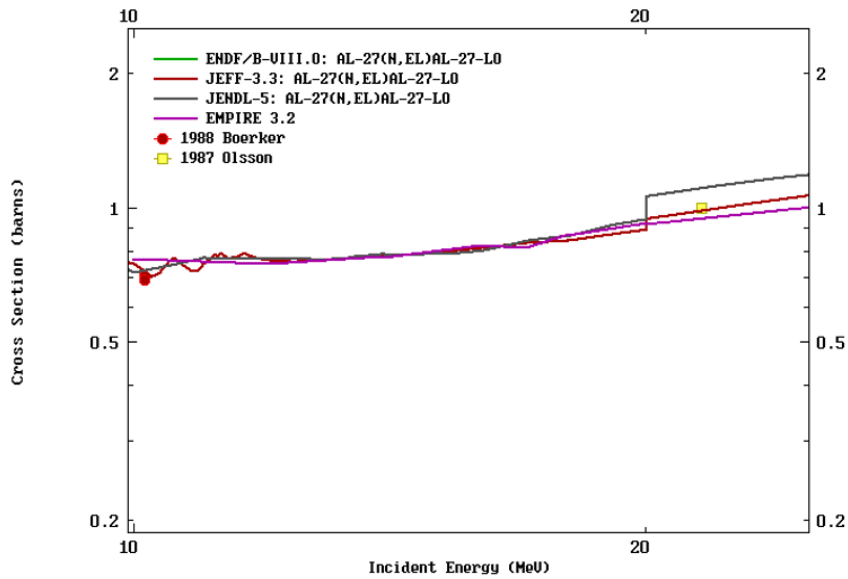


Figure 2. Calculated reaction cross-section with EMPIRE 3.2 on  $^{27}\text{Al}(n,el)$  in comparisons with the measured data and evaluated data

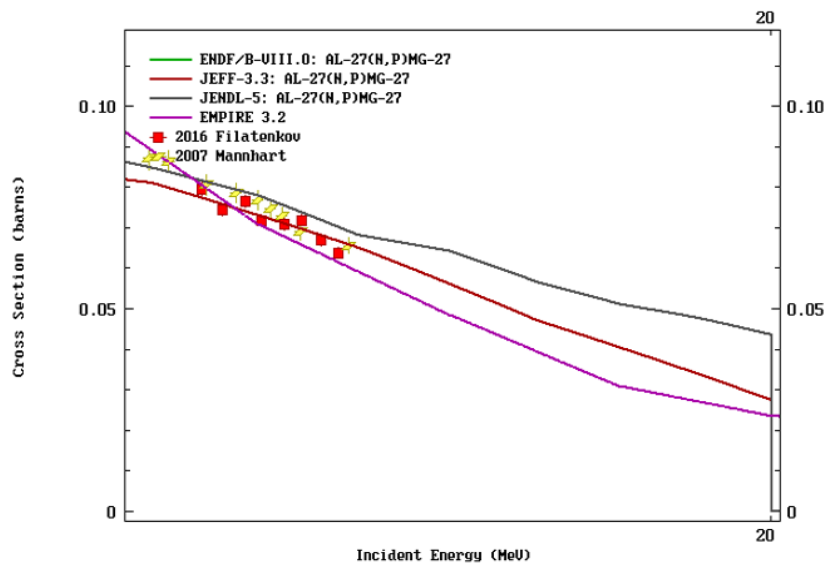


Figure 3. Calculated reaction cross-section with EMPIRE 3.2.3 on  $^{27}\text{Al}(n,p)$  in comparisons with the measured data and recent evaluated data

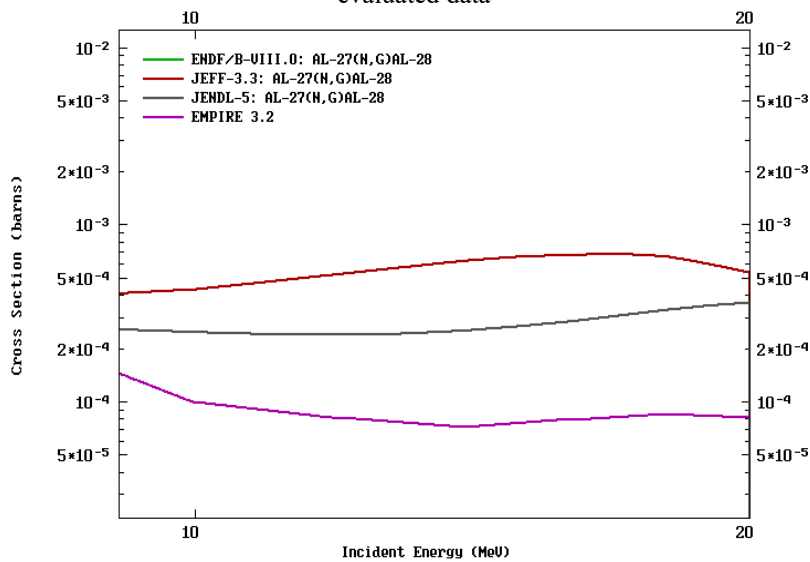
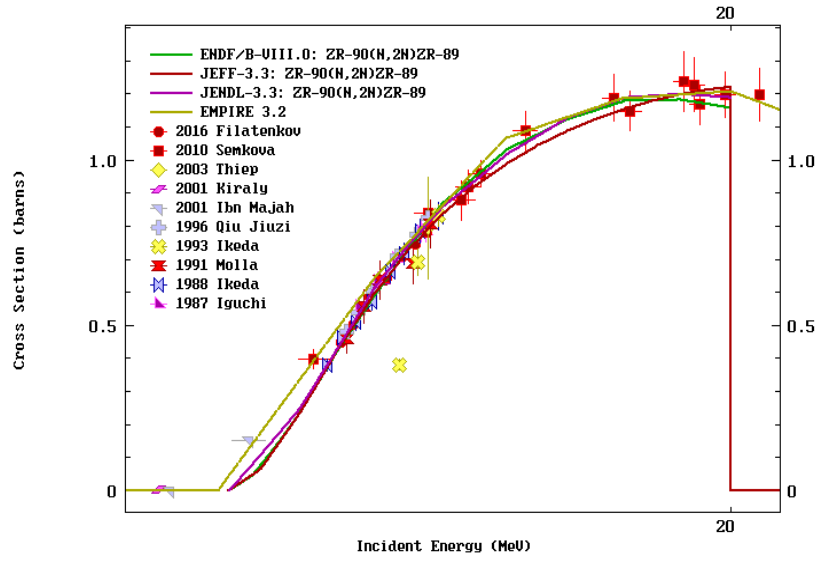
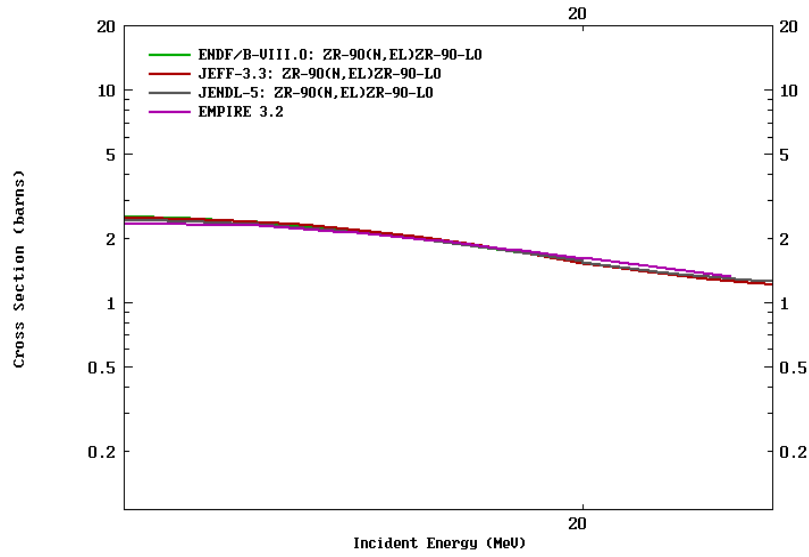


Figure 4. Calculated reaction cross-section with EMPIRE 3.2.3 on  $^{27}\text{Al}(n,\gamma)$  in comparisons with the evaluated data



**Figure 5.** Calculated reaction cross-section with EMPIRE 3.2.3 on  $^{90}\text{Zr}(n, 2n)$  in comparisons with the measured data and recent evaluated nuclear data



**Figure 6.** Calculated reaction cross-section with EMPIRE 3.2.3 on  $^{90}\text{Zr}(n, el)$  in comparisons with evaluated nuclear data

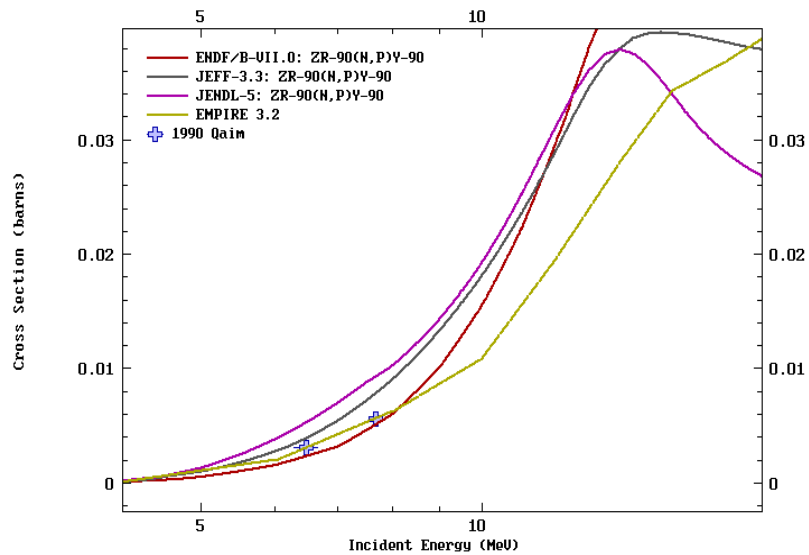


**Figure 7.** Calculated reaction cross-section with EMPIRE 3.2 on  $^{90}\text{Zr}(n, p)$  in comparisons with the measured data evaluated nuclear data

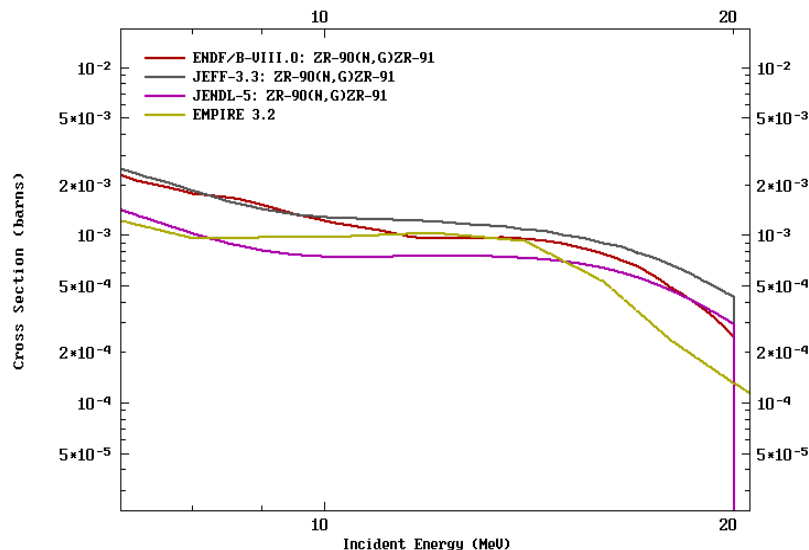


**Figure 8.** Calculated reaction cross-section with EMPIRE 3.2.3 on  $^{27}\text{Al}(n, \gamma)$  in comparison with evaluated nuclear data

The results of  $^{90}\text{Zr}(n, 2n)$ ,  $^{90}\text{Zr}(n, el)$ ,  $^{90}\text{Zr}(n, p)$  and  $^{90}\text{Zr}(n, \gamma)$  cross section was displayed Figures 5-8. Theoretical calculation of  $^{90}\text{Zr}(n, 2n)$  with EMPIRE 3.2.3 is in good agreement with the evaluated nuclear data and the experimental data retrieved from EXFOR [23] as shown in the Figure 5. The response of cross section in the graph increases with increase in neutron incident energy. The neutron induced reaction of  $^{90}\text{Zr}(n, el)$  cross section decreases slowly with increase in incident neutron energy as shown in Figure 6. But our results are in good harmony with existing evaluated data. In Figure 7, EMPIRE 3.2.3 results on  $^{90}\text{Zr}(n, p)$  reproduce the measurement data [24, 25], better than other evaluated nuclear data. In the graph, the cross section increases sharply at  $E_n \geq 5 \text{ MeV}$  with the increase in incident neutron energy; and discrepancy of 4.2% exists between this work and existing evaluated nuclear data at  $E_n \geq 10 \text{ MeV}$ . The neutron induced

cross section of  $^{90}\text{Zr}(n, g)^{90}\text{Zr}$  almost constant with increase in neutron energy up to 15 MeV, Above this energy, cross section decreases slowly until it fall suddenly at 20 MeV. as shown in Figure 8. The variation between our calculated results and evaluated nuclear data which may likely has to do with model deficiency since there was no reported experimental data to constrain the model.

#### 4. COMPARISON OF NEUTRON – INDUCED REACTION CROSS-SECTION BETWEEN $^{27}\text{Al}$ TARGET AND THE $^{90}\text{Zr}$ TARGET

Theoretical calculated of  $^{27}\text{Al}$  target in comparison with  $^{90}\text{Zr}$  target is displayed in the numerical form as seen in Table 2 in the energy region of  $E_n = 10 - 25 \text{ MeV}$ .

**Table 2.** Comparison of neutron induced reaction cross-section of zirconium and aluminum target

E MeV	$^{90}\text{Zr}(n, 2n)$ (mb)	$^{27}\text{Al}(n, 2n)$ (mb)	$^{90}\text{Zr}(n, el)$ (mb)	$^{27}\text{Al}(n, el)$ (mb)	$^{90}\text{Zr}(n, p)$ (mb)	$^{27}\text{Al}(n, p)$ (mb)	$^{90}\text{Zr}(n, \gamma)$ (mb)	$^{27}\text{Al}(n, \gamma)$ (mb)
10	0.00	0.00	2354.4	766.7	28.7	95.8	1.28	0.096
12	0.00	0.00	2301.3	752.3	46.1	103.2	0.83	0.081
14	639.2	2.4	2152.2	776.1	58.9	70.7	0.62	0.073
16	1067.9	57.9	1963.9	818.7	53.2	48.5	0.36	0.080
18	1189.5	104.1	1775.7	869.5	44.9	30.8	0.19	0.084
20	1207.2	124.7	160.88	922.1	42.3	23.5	0.12	0.083
25	995.3	56.1	1333.7	998.0	33.4	11.0	0.04	0.043

It is clearly seen in the table that reaction cross section of  $^{90}\text{Zr}$  target have higher absorption cross section compares to the  $^{27}\text{Al}$  target. But between 10- 14 MeV incident energy, the cross section on  $^{27}\text{Al}(n, p)$  target is great than that of  $^{90}\text{Zr}(n, p)$ .

#### 5. CONCLUSION

NIRR-1 is a research reactor and has been used for different purposes since the advent of this technology. Initially, NIRR-1 uses highly enriched Uranium as a fuel (HEU) with aluminum as cladding material. To address the proliferation-related issue, the HEL fuel was replaced with LEU and other compartments with Zirconium alloy as a cladding. In order to

have a comprehensive knowledge of the replaced cladding materials, we model the target of interest using the statistical nuclear reaction code EMPIRE 3.2.3 code. Different parameters were tested within the optical model, pre-equilibrium and compound model to obtain a good cross-section in agreement with standard data, and available measured data were retrieved from EXFOR. Our calculation shows a reasonable agreement with measured data but a large variation was observed between the EMPIRE calculation and the existing evaluated nuclear data file, most especially in  $(n, p)$  and  $(n, \gamma)$  channel which may likely link to model deficiency as a result of a scarcity of experimental reasonable data to constrained the model.

The obtained values of reaction cross section on Zr target were compared with Al target in all reaction channels of

interest as presented in Table 2. It is seen that the numerical value of the zirconium cross section is higher than that of the aluminum cross section which makes zirconium a preferred cladding material. New cross section was provided in the energy region where experimental data is scarce. This provides a confident in theoretical model EMPIRE 3.2.3 code in calculation of cross section and to update the nuclear data for nuclear applications. However, new experimental data is needed to assess current data in most discrepant evaluation regions.

## REFERENCES

- [1] Jonah, S.A., Ibrahim, Y.V., Ajuji, A.S., Onimisi, M.Y. (2012). The impact of HEU to LEU conversion of commercial MNSR: Determination of neutron spectrum parameters in irradiation channels of NIRR-1 using MCNP code. *Annals of Nuclear Energy*, 39(1): 15-17. <https://doi.org/10.1016/j.anucene.2011.08.026>
- [2] Jonah, S.A., Balogun, G.I., Umar, I.M., Mayaki, M.C. (2005). Neutron spectrum parameters in irradiation channels of the Nigeria Research Reactor-1 (NIRR-1) for the k 0-NAA standardization. *Journal of Radioanalytical and Nuclear Chemistry*, 266: 83-88. <https://doi.org/10.1007/s10967-005-0873-8>
- [3] Adeoti, O.M., Dahunsi, O.A., Awopetu, O.O., Oladosu, K.O., Ikumapayi, O.M. (2019). Optimization of clay-bonded graphite crucible using D-optimal design under mixture methodology. *International Journal of Scientific & Technology Research*, 8(7): 444-461.
- [4] Koning, A.J., Delaroche, J.P. (2003). Local and global nucleon optical models from 1 keV to 200 MeV. *Nuclear Physics A*, 713(3-4): 231-310. [https://doi.org/10.1016/S0375-9474\(02\)01321-0](https://doi.org/10.1016/S0375-9474(02)01321-0)
- [5] Simon, J.O.H.N., Ibrahim, Y.V., Adeyemo, D.J., Garba, N.N., Asuku, A., Bello, S., Ibikunle, I.K. (2022). Radiological consequence analysis for hypothetical accidental release from Nigerian Research Reactor-1. *Applied Radiation and Isotopes*, 186: 110308. <https://doi.org/10.1016/j.apradiso.2022.110308>
- [6] Herman, M., Capote, R., Carlson, B. V., Obložinský, P., Sin, M., Trkov, A., Wienke, H., Zerkin, V. (2007). EMPIRE: Nuclear reaction model code system for data evaluation. *Nuclear Data Sheets*, 108(12): 2655-2715. <https://doi.org/10.1016/j.nds.2007.11.003>
- [7] Jonah, S.A., Umar, I.M., Oladipo, M.O.A., Balogun, G.I., Adeyemo, D.J. (2006). Standardization of NIRR-1 irradiation and counting facilities for instrumental neutron activation analysis. *Applied Radiation and Isotopes*, 64(7): 818-822. <https://doi.org/10.1016/j.apradiso.2006.01.012>
- [8] Brown, D.A., Chadwick, M.B., Capote, R., et al. (2018). ENDF/B-VIII. 0: The 8th major release of the nuclear reaction data library with CIELO-project cross sections, new standards and thermal scattering data. *Nuclear Data Sheets*, 148: 1-142. <https://doi.org/10.1016/j.nds.2018.02.001>
- [9] Jonah, S.A., Ibrahim, Y.V., Akaho, E.H.K. (2008). The determination of reactor neutron spectrum-averaged cross-sections in miniature neutron source reactor facility. *Applied Radiation and Isotopes*, 66(10): 1377-1380. <https://doi.org/10.1016/j.apradiso.2008.04.001>
- [10] Capote, R., Herman, M., Obložinský, P., et al. (2009). RIPL—reference input parameter library for calculation of nuclear reactions and nuclear data evaluations. *Nuclear Data Sheets*, 110(12): 3107-3214. <https://doi.org/10.1016/j.nds.2009.10.004>
- [11] Olorunsola, A.B., Ikumapayi, O.M., Oladapo, B.I., Alimi, A.O., Adeoye, A.O.M. (2021). Temporal variation of exposure from radio-frequency electromagnetic fields around mobile communication base stations. *Scientific African*, 12: e00724. <https://doi.org/10.1016/j.sciaf.2021.e00724>
- [12] Kalbach, C. (1977). The Griffin model, complex particles and direct nuclear reactions. *Zeitschrift für Physik A Atoms and Nuclei*, 283(4): 401-411. <https://doi.org/10.1007/BF01409522>
- [13] Plompen, A.J., Cabellos, O., De Saint Jean, C., et al. (2020). The joint evaluated fission and fusion nuclear data library, JEFF-3.3. *The European Physical Journal A*, 56: 1-108. <https://doi.org/10.1140/epja/s10050-020-00141-9>
- [14] Taova, S., Otuka, N. (2015). International Network of Nuclear Reaction Data Centres (NRDC) (No. indc-nds-0686). NA. <https://nds.iaea.org/publications/indc/indc-nds-0686/>
- [15] Ikumapayi, O.M., Attah, B.I., Afolabi, S.O., Adeoti, O.M., Bodunde, O.P., Akinlabi, S.A., Akinlabi, E.T. (2020). Numerical modelling and mechanical characterization of pure aluminium 1050 wire drawing for symmetric and axisymmetric plane deformations. *Mathematical Modelling of Engineering Problems*, 7(4): 539-548. <https://doi.org/10.18280/mmep.070405>
- [16] Filatenkov, A.A. (2016). Neutron activation cross sections measured at KRI in neutron energy region 13.4–14.9 MeV. USSR report to the INDC. No. 0460, Austria.
- [17] Attar, F.M.D., Bholane, G.T., Ganesapandy, T.S., Dhole, S.D., Bhoraskar, V.N. (2022). Isomeric cross sections of the (n,  $\alpha$ ) reactions on the  $^{90}\text{Zr}$ ,  $^{93}\text{Nb}$  and  $^{92}\text{Mo}$  isotopes measured for 13.73 MeV–14.77 MeV and estimated for 10 MeV–20 MeV neutron energies. *Applied Radiation and Isotopes*, 184: 110192. <https://doi.org/10.1016/j.apradiso.2022.110192>
- [18] Sudbrock, F., Herpers, U., Qaim, S.M., Csikai, J., Kubik, P.W., Synal, H.A., Suter, M. (2000). Cross sections for the formation of long-lived radionuclides  $^{10}\text{Be}$ ,  $^{26}\text{Al}$  and  $^{36}\text{Cl}$  in 14.6 MeV neutron induced reactions determined via accelerator mass spectrometry (AMS). *Radiochimica Acta*, 88(12): 829-832. <https://doi.org/10.1524/ract.2000.88.12.829>
- [19] Börker, G., Boettger, R., Brede, H.J., Klein, H., Mannhart, W., Siebert, B.R.L. (1989). Elastic and inelastic differential neutron scattering cross sections of oxygen between 6 and 15 meV (No. PTB-N--1). *Physikalisch-Technische Bundesanstalt*. [https://inis.iaea.org/search/search.aspx?orig\\_q=RN:21022544](https://inis.iaea.org/search/search.aspx?orig_q=RN:21022544)
- [20] Olsson, N., Trostell, B., Ramström, E., Holmqvist, B., Dietrich, F.S. (1987). Microscopic and conventional optical model analysis of neutron elastic scattering at 21.6 MeV over a wide mass range. *Nuclear Physics A*, 472(2): 237-268. [https://doi.org/10.1016/0375-9474\(87\)90209-0](https://doi.org/10.1016/0375-9474(87)90209-0)
- [21] Kiraly, B., Csikai, J., Doczi, R. (2001). Validation of neutron data libraries by differential and integral cross sections. *JAERI Conference Proceedings*, 283-288. <https://www.osti.gov/etdeweb/biblio/20233170>

- [22] Mannhart, W., Schmidt, D. (2007). Measurement of neutron activation cross sections in the energy range from 8 MeV to 15 MeV, Physikalisch-Technische Bundesanstalt, Braunschweig (Germany) Neutronenphysik. PTB Report PTB-N-53.
- [23] Majah, M.I., Chiadli, A., Sudár, S., Qaim, S.M. (2001). Cross sections of (n, p), (n,  $\alpha$ ) and (n, 2n) reactions on some isotopes of zirconium in the neutron energy range of 10-12 MeV and integral tests of differential cross section data using a 14 MeV d (Be) neutron spectrum. *Applied Radiation and Isotopes*, 54(4): 655-662. [https://doi.org/10.1016/S0969-8043\(00\)00299-2](https://doi.org/10.1016/S0969-8043(00)00299-2)
- [24] Qaim, S.M., Majah, M.I., Wölfle, R., Strohmaier, B. (1990). Excitation functions and isomeric cross-section ratios for the Zr 90 (n, p) 90 Y m, g and Zr 91 (n, p) 91 Y m, g processes. *Physical Review C*, 42(1): 363. <https://doi.org/10.1103/PhysRevC.42.363>
- [25] Li, Y., Song, Y., Zhou, F., Chang, X., Zhang, X., Tian, M., Yuan, S. (2020). Cross section measurements on zirconium isotopes for ~ 14 MeV neutrons and their theoretical calculations of excitation functions. *Chinese Physics C*, 44(12): 124001. <https://doi.org/10.1088/1674-1137/abb4d3>